Received: 18 October 2023 | Accepted: 21 April 2024

DOI: 10.1097/HC9.0000000000000474

ORIGINAL ARTICLE

OPEN

Hepatocyte-specific loss of DDB1 attenuates hepatic steatosis but aggravates liver inflammation and fibrosis in MASH

Qiuxia Gu[1,2,3] | **Yushun Chang**[1,2] | **Yan Jin**[1] | **Jing Fang**[1,2,3] | **Tong Ji**[1,2] | **Jie Lin**[1,2] | **Xi Zhu**[1] | **Binzhi Dong**[1,3] | **Hanning Ying**[1,3] | **Xiaoxiao Fan**[1] | **Zheyong Li**[1,3] | **Zerui Gao**[4] | **Yongfen Zhu**[1,3,5] | **Yifan Tong**[1,3] | **Xiujun Cai**[1,2]

[1]Department of General Surgery, Sir Run Run Shaw Hospital, Zhejiang University School of Medicine, Hangzhou, China

[2]Zhejiang Provincial Key Laboratory of Laparoscopic Technology, Sir Run Run Shaw Hospital, Zhejiang University School of Medicine, Hangzhou, China

[3]Liver Regeneration and Metabolism Study Group, Sir Run Run Shaw Hospital, Zhejiang University School of Medicine, Hangzhou, China

[4]Zhejiang University School of Medicine, Hangzhou, Zhejiang, China

[5]Department of Infectious Diseases, Sir Run Run Shaw Hospital, Zhejiang University School of Medicine, Hangzhou, China

Correspondence
Yongfen Zhu, Department of Infectious Diseases, Sir Run Run Shaw Hospital, Zhejiang University School of Medicine, Hangzhou 310016, China.
Email: yongfenzhu@zju.edu.cn

Yifan Tong, Department of General Surgery, Sir Run Run Shaw Hospital, Zhejiang University School of Medicine, Hangzhou 310016, China.
Email: tongyf@zju.edu.cn

Xiujun Cai, Department of General Surgery, Sir Run Run Shaw Hospital, Zhejiang University School of Medicine, Hangzhou 310016, China.
Email: srrsh_cxj@zju.edu.cn

Abstract

Background: MASH is a common clinical disease that can lead to advanced liver conditions, but no approved pharmacotherapies are available due to an incomplete understanding of its pathogenesis. Damaged DNA binding protein 1 (DDB1) participates in lipid metabolism. Nevertheless, the function of DDB1 in MASH is unclear.

Methods: Clinical liver samples were obtained from patients with MASH and control individuals by liver biopsy. Hepatocyte-specific *Ddb1*-knockout mice and liver *Hmgb1* knockdown mice were fed with a methionine-and choline-deficient diet to induce MASH.

Results: We found that the expression of DDB1 in the liver was significantly decreased in MASH models. Hepatocyte-specific ablation of DDB1 markedly alleviated methionine-and choline-deficient diet-induced liver steatosis but unexpectedly exacerbated inflammation and fibrosis. Mechanistically, DDB1 deficiency attenuated hepatic steatosis by downregulating the expression of lipid synthesis and uptake genes. We identified high-mobility group box 1 as a key candidate target for DDB1-mediated liver injury. DDB1 deficiency upregulated the expression and extracellular release of high-mobility group box 1, which further increased macrophage infiltration and activated HSCs, ultimately leading to the exacerbation of liver inflammation and fibrosis.

Abbreviations: AAV8, adeno-associated virus 8; ALT, alanine aminotransferase; AST, aspartate aminotransferase; DDB1, damaged DNA binding protein 1; GSEA, gene set enrichment analysis; HMGB1, high-mobility group box 1; LKO, hepatocyte-specific knockout; MCD, methionine/choline-deficient diet; OA, oleic acid; OE, overexpression; PA, palmitic acid; PPARg, peroxisome proliferator-activated receptor gamma; SCD, standard control diet; TG, triglyceride; WT, wild type.

Qiuxia Gu, Yushun Chang, and Yan Jin contributed equally to this work.

Supplemental Digital Content is available for this article. Direct URL citations are provided in the HTML and PDF versions of this article on the journal's website, www.hepcommjournal.com.

Conclusions: These data demonstrate the independent regulation of hepatic steatosis and injury in MASH. These findings have considerable clinical implications for the development of therapeutic strategies for MASH.

INTRODUCTION

MASLD is rapidly becoming the most prevalent chronic liver disease, affecting up to 25% of the population in the world.[1–3] MASLD includes a range of liver abnormalities, from simple hepatic steatosis to MASH characterized by hepatocellular damage, lobular inflammation, and even liver fibrosis.[4] MASH can ultimately lead to liver cirrhosis and HCC.[5] Given its complexity and heterogeneity, no approved pharmacotherapies are available for clinical use.[6] Therefore, it is critical to clarify the pathophysiology of MASH and pinpoint effective therapeutic targets or approaches to treatment.

Damaged DNA binding protein 1 (DDB1) was initially identified as a component of the heterodimeric complex (DDB1/DDB2), which binds to UV-damaged DNA.[7] This protein is now identified as a scaffolding protein in the Cullin4-RING E3 ubiquitin ligase, which regulates the ubiquitination and degradation of several proteins.[8] In addition, DDB1 is a molecular partner of transcription factors that regulates the transcription of multiple genes.[9,10] In summary, DDB1 regulates various biological processes, such as DNA repair, gene transcription, and cell cycling.[11] Intriguingly, it has been revealed that DDB1 is essential for glucose metabolism in the mammalian liver.[12] Moreover, 2 recent researches have shown that DDB1 is critically involved in lipid metabolism, including adipogenesis and the onset of obesity.[13,14] However, the function of DDB1 in the pathogenesis of MASH remains unclear.

In this study, we identified that DDB1 was significantly decreased during MASH progression. Hepatic steatosis was alleviated by hepatocyte-specific DDB1 knockout, which was associated with the downregulation of lipogenic gene expression. Unexpectedly, DDB1 ablation significantly exacerbated liver injury and fibrosis. Mechanistically, DDB1 deficiency upregulated the expression and extracellular release of high-mobility group box 1 (HMGB1). HMGB1 acts as a prototypical damage-associated molecular pattern, further increases macrophage infiltration, and activates HSCs, ultimately exacerbating liver inflammation and fibrosis. Our findings uncover a previously unknown role of DDB1 in liver steatosis, inflammation, and fibrosis.

METHODS

Human liver samples

Clinical liver samples were obtained from patients by liver biopsy at Sir Run Run Shaw Hospital, Zhejiang University. Each patient provided informed consent for tissue analysis. Pathologists evaluated and scored the histological slides as MASLD, MASH, or normal liver (the presence of steatosis <5%) based on the steatosis/activity/fibrosis score.[15] Snap-frozen fresh liver tissues were then used for western blot analysis. All procedures involving human samples conformed to the principles of the Declaration of Helsinki and were approved by the Institutional Review Board of the Sir Run Run Shaw Hospital, Zhejiang University.

Animal models and treatments

Ddb1$^{flox/flox}$ mice were obtained from Prof Yong Cang of Shanghai Tech University and were hybridized with Albumin-Cre$^{+/-}$ mice to generate hepatocyte-specific *Ddb1*-knockout (*Ddb1*-LKO) mice. The liver *Hmgb1* knockdown mouse model and the control were generated by i.v. injection of adeno-associated virus 8 expressing shRNA against *Hmgb1* (AAV8-shHmgb1; HANBIO) and AAV8-shNC (negative control), respectively. Liver samples from leptin receptor deletion mice (db/db) and control group (db/m) were gifted by Prof Zheng Fenping of Zhejiang University. The mice were kept in a controlled environment (23°C ± 2°C, 12 h of light/dark cycle). Six-week-old male mice were fed a methionine/choline-deficient diet (MCD; TP3005G; Trophic Diet) for 4 weeks to induce MASH. Mice fed a standard control diet (SCD; D12450B; Research Diets) served as controls. All animal procedures were approved by the Animal Ethics Committee of Zhejiang University and conformed to the National Institutes of Health (NIH) guidelines.

Histological analysis and immunohistochemistry

The livers of mice were harvested and weighed for further analysis. Mouse livers were fixed in 4% formaldehyde or Tissue-Tek OCT compound for the preparation of paraffin sections and frozen sections, respectively. Paraffin sections were stained with hematoxylin and eosin, Sirius Red, and immunohistochemical. Oil red O (G1263; Solarbio) staining was performed on frozen sections to identify lipid droplets. The primary antibodies used are listed in Supplemental Table S1, http://links.lww.com/HC9/A940. According to the MASLD Activity Score, the

steatosis, lobular inflammation, and ballooning change of the mouse liver were evaluated. MASH is defined as the presence of steatosis in > 5% of hepatocytes, along with any degree of hepatocyte ballooning and any amount of lobular inflammation.[15]

Primary hepatocyte isolation

Mouse hepatocytes were isolated as reported.[16] In brief, anesthetized mice were perfused with buffer solution through the IVC. After being digested, the livers were suspended in sterilized PBS and filtered. Hepatocytes were then isolated by centrifugation and cultured in dishes covered with 50 μg/mL collagen type I.

Plasmids, lentivirus production, and stable cell lines

The full-length CDS of the human DDB1 gene was amplified and recombined with the PCDH vector for overexpression of DDB1 (DDB1-OE) according to the protocol. ShRNA targeting the human DDB1 gene (shDDB1) was designed and constructed into the Phy-304 vector. The sequence used to build plasmids is listed in Supplemental Table S1, http://links.lww.com/HC9/A940. Lentiviruses were packaged in 293T cells using a dual-packaging plasmid system (pMD2.G, psPAX2). After lentivirus infection of the HepG2 cells, stably transformed cell lines were selected with puromycin.

Cell culture and treatments

The human HepG2 cell line was acquired from the Chinese Academy of Sciences. HepG2 cells and primary murine hepatocytes were incubated in DMEM Gibco) supplemented with 10% fetal bovine serum (Gibco) in a 37°C incubator containing 5% carbon dioxide. To induce the lipid accumulation model in vitro, the cells were starved with serum-free DMEM containing 1% bovine serum albumin (Fdbio Science) for 16 hours and treated with 0.5 mM oleic acid (OA; O1383; Sigma-Aldrich) for another 24 hours.

Hepatic triglycerides and serum biochemistry

Hepatic triglycerides (TGs) were extracted and analyzed with a Triglyceride Content Assay Kit (E1013; Applygen). Serum alanine aminotransferase (ALT) and aspartate aminotransferase (AST) levels were measured using the ALT assay kit and AST assay kit (Nanjing Jiancheng). Serum and supernatant HMGB1 concentrations were measured using an ELISA kit (44107M1; Meimian).

CCK8 assay

Cell viability was evaluated using a Cell Counting Kit (CCK8; Yeasen). Approximately 5×10^8/L cells were seeded in 96-well plates in 100 μL per well. After cell starvation, different concentrations of OA were added and incubated for 24 hours. The cells were treated with 10 μL of CCK8 solution, and after 45 minutes, the OD values were measured by the microplate reader (Thermo Scientific) at 450 nm.

Western blotting

The nuclear and cytoplasmic proteins were isolated using the PARIS Kit (Thermo Scientific). Total proteins from tissues or cells were extracted by radioimmunoprecipitation assay lysis buffer supplemented with proteinase inhibitors and quantified with the bicinchoninic acid protein assay kit (Thermo Scientific). Proteins were separated on 10%–12% sodium dodecyl sulfate-polyacrylamide gels and transferred to polyvinylidene fluoride membranes. After 1 hour of blocking, the membranes were incubated overnight with the primary antibody and an additional hour with the corresponding secondary antibody. The blots were visualized using an enhanced chemiluminescence system (Bio-Rad). The antibodies are listed in Supplemental Table S1, http://links.lww.com/HC9/A940.

Quantitative real-time PCR

Total RNA was isolated from liver tissues or cultured cells using TRIzol reagent (Invitrogen). Two micrograms of RNA were reverse-transcribed into cDNA with the cDNA synthesis kit (11123ES60; Yeasen). Quantitative real-time PCR was performed using the SYBR Green Master Mix kit (11198ES08; Yeasen). The levels of target mRNA expression were normalized to the expression of β-actin. The primers are listed in Supplemental Table S1, http://links.lww.com/HC9/A940.

RNA sequencing and data analysis

Total RNA was extracted from mouse liver tissues using TRIzol reagent (Invitrogen), and RNA quality was evaluated. The RNA libraries were sequenced on the Illumina NovaseqTM 6000 platform by OE Biotech, Inc. Gene set enrichment analysis (GSEA) was conducted

utilizing the Java GSEA platform. A predefined gene set was employed for the analysis, and the genes were ranked based on the degree of differential expression between the 2 sample types.

Statistical analysis

Statistical analyses were performed using GraphPad Prism 9.0 software. Student *t* test was used to detect differences between the 2 groups, while ANOVA was applied for comparisons among the various treatments. All values are shown as the mean ± SD. Differences with a *p* value of <0.05 were deemed statistically significant. *$p < 0.05$, **$p < 0.01$, and ***$p < 0.001$.

RESULTS

DDB1 is downregulated in patients with MASH and murine models

To explore the mechanism of MASH progression, we initially performed RNA sequencing on the livers of mice with MCD-induced MASH (Supplemental Figures S1A–F, http://links.lww.com/HC9/A940). The volcano plot demonstrated that, in mice fed MCD as opposed to SCD, *Ddb1* was a significantly downregulated gene (Figures 1A, B). The mRNA and protein levels of DDB1 in MCD-fed mice were also decreased compared with those in SCD-fed mice (Figure 1C, Supplemental Figure S1G, http://links.lww.com/HC9/A940). We further measured the expression of DDB1 in db/db and db/m mice, which are common monogenic obesity animals with fatty livers and their corresponding controls.[17] Distinct downregulation of DDB1 expression (Figure 1D, Supplemental Figure S1H, http://links.lww.com/HC9/A940) was consistently detected in db/db mouse livers. In addition, we examined the expression of DDB1 in normal and MASH human livers. Compared with those in normal livers, the mRNA and protein levels of DDB1 were markedly reduced in the livers of individuals with MASH (Figure 1E, Supplemental Figure S1I, http://links.lww.com/HC9/A940). Correspondingly, immunohistochemical staining showed that hepatocyte DDB1 protein levels were reduced in both patients with MASH and murine MASH models (Figure 1F). Taken together, these results suggest that DDB1 is involved in the pathogenesis of MASH.

DDB1 aggravates lipid accumulation but suppresses damage to hepatocytes

We further investigated the functional roles of DDB1 in MASH by challenging hepatocytes with OA in vitro (Supplemental Figures S2A–E, http://links.lww.com/HC9/A940). We constructed DDB1 knockdown and overexpressing HepG2 cell lines (Figure 2A, Supplemental Figures S2F, G, http://links.lww.com/HC9/A940). Compared with those in the control group, silencing DDB1 prominently inhibited OA-induced lipid accumulation and significantly reduced cellular TG levels (Figures 2B–D). In addition, we supplemented the cells with a combination of OA and palmitic acid at a ratio of 1:1 and a concentration of 0.5 mM for 24 hours. The results showed that there was no significant difference in lipid deposition and cell viability compared with the OA treatment group (Supplemental Figures S2H, I, http://links.lww.com/HC9/A940). Furthermore, DDB1 silencing inhibited the expression of genes related to lipogenesis (FASN [fatty acid synthase], SCD1 [stearoylCoA desaturase 1], and PPARg) and lipid uptake (CD36 [cluster of differentiation 36]) (Supplemental Figure S2J, http://links.lww.com/HC9/A940). In contrast, DDB1-OE markedly promoted OA-induced lipid deposition and upregulated the expression of genes associated with lipid metabolism (Figures 2B, F, G, Supplemental Figure S2K, http://links.lww.com/HC9/A940). However, we found that the viability of shDDB1 HepG2 cells significantly declined in response to different concentrations of OA, while the viability of DDB1-OE cells was increased (Figures 2E, H). We further obtained *Ddb1*-LKO mice and isolated primary hepatocytes from LKO and littermate wild-type (WT) mice. Western blotting and qPCR were performed to ensure tissue-specific knockout of *Ddb1* (Supplemental Figures S3A–C, http://links.lww.com/HC9/A940). After OA stimulation, the lipid droplets and cellular TG content of DDB1-deficient primary hepatocytes were much higher than those of the control, but cell viability was also significantly reduced (Figures 1I–L). Collectively, these data show that DDB1 can aggravate lipid accumulation but suppresses damage in hepatocytes.

Hepatocyte-specific DDB1 deficiency attenuates MCD-induced hepatic steatosis but exacerbates liver injury

Next, we attempted to explore the role of DDB1 in MASH in vivo. LKO and WT mice were fed an SCD or MCD for 4 continuous weeks. MCD-fed mice exhibited vigorous body weight loss compared with SCD-fed mice, but there was no comparable difference between LKO and WT mice after MCD feeding (Supplemental Figure S3D, http://links.lww.com/HC9/A940). However, the liver weight and liver-weight-to-body-weight ratio were markedly lower in LKO mice than in WT mice after MCD consumption (Supplemental Figures S3E, F, http://links.lww.com/HC9/A940). Similarly, liver TG levels were notably reduced in MCD-fed LKO mice (Figure 3A). Hematoxylin and eosin and Oil red O staining indicated that liver lipid accumulation and

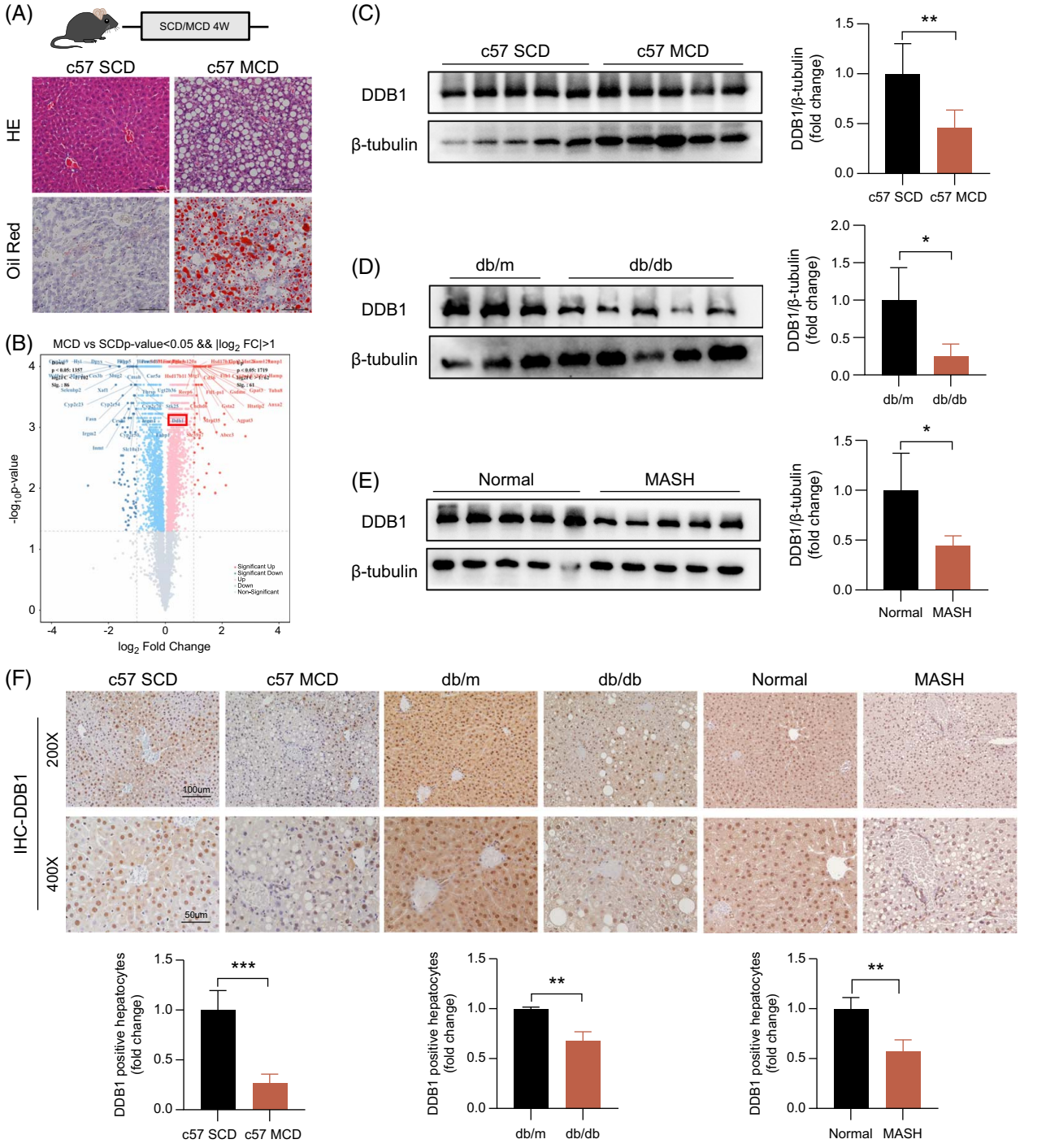

FIGURE 1 DDB1 is downregulated in MASH patients and murine models. (A, B) The volcano plot of RNA sequencing on the livers of mice fed with SCD or MCD for 4 weeks (n = 5 mice per group). (C) DDB1 protein levels in C57BL/6 mice fed the SCD or MCD (n = 5 per group). (D) DDB1 protein levels in genetically obese (db/db) mice and control (db/m) mice (n = 3 in db/m and n = 5 in db/db group). (E) Hepatic DDB1 western blot of DDB1 protein levels in liver tissues from normal donors (no steatosis) and patients with MASH (n = 5 individuals in each group). (F) Representative IHC staining was applied to detect the DDB1 expression in the livers of patients with MASH, db/db mice, or MCD-induced mice and their corresponding controls (n = 4 per group). All data are presented as the mean ± SD, *$p < 0.05$, **$p < 0.01$, ***$p < 0.001$. Abbreviations: DDB1, damaged DNA binding protein 1; IHC, immunohistochemical; MCD, methionine-and choline-deficient diet; SCD, standard control diet.

steatosis were attenuated in LKO mice after MCD feeding (Figure 3D, E). Unexpectedly, the serum concentrations of ALT and AST were significantly increased in MCD-fed LKO mice (Figures 3B, C). Elevated liver enzymes in the presence of improved steatosis suggested a possible dissociation between the reduction in steatosis and the worsening of liver injury. We further analyzed the role of DDB1 on liver inflammation and fibrosis. After 4 weeks of MCD feeding, LKO mice showed worsened lobular

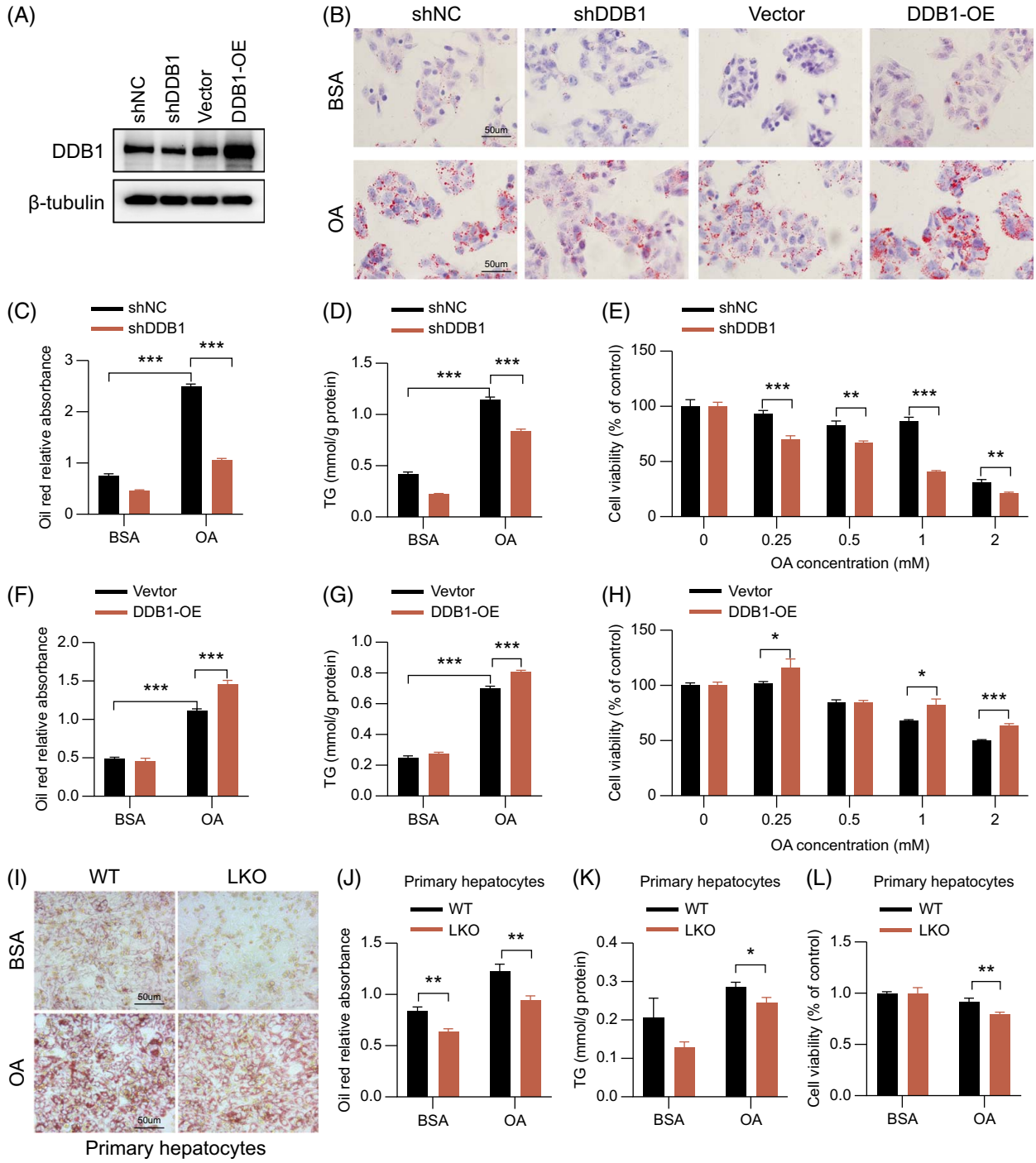

FIGURE 2 DDB1 aggravates lipid accumulation but suppresses damage in hepatocytes. (A) Western blot analysis of DDB1 expression in HepG2 cells transfected with shDDB1 or DDB1-OE plasmid and their controls. (B) Representative ORO staining of HepG2 cells in DDB1 knockdown or overexpressing and their control groups stimulated with BSA or OA (0.5 mM) for 24 hours. Scale bar, 50 μm. (C, F) Quantitative analysis of ORO staining. (D, G) The cellular contents of TG in the indicated HepG2 cell groups were stimulated with BSA or OA (0.5 mM) for 24 hours. (E, H) CCK8 analysis of HepG2 cell viability in the indicated groups stimulated with different OA concentrations (0, 0.25, 0.5, 1, and 2 mM) for 24 hours. (I) Representative ORO staining of primary hepatocytes stimulated with BSA or OA (0.5 mM) for 24 hours. Scale bar, 50 μm. (J) Quantitative analysis of ORO staining. (K) The cellular contents of TG in the indicated primary hepatocyte group. (L) CCK8 analysis of primary hepatocyte viability in the indicated groups. All data are presented as the mean ± SD, $^{*}p < 0.05$, $^{**}p < 0.01$, $^{***}p < 0.001$. Abbreviations: BSA, bovine serum albumin; DDB1, damaged DNA binding protein 1; OA, oleic acid; ORO, Oil red O; TG, triglyceride.

inflammation and hepatocyte ballooning according to MASLD Activity Scores (Figures 3D, E). Liver F4/80 staining showed increased macrophage infiltration in MCD-fed LKO mice. Moreover, alpha smooth muscle actin staining demonstrated that DDB1 deficiency activated HSCs and aggravated MCD-induced fibrosis, which was consistent with Sirius Red staining (Figure 3E).

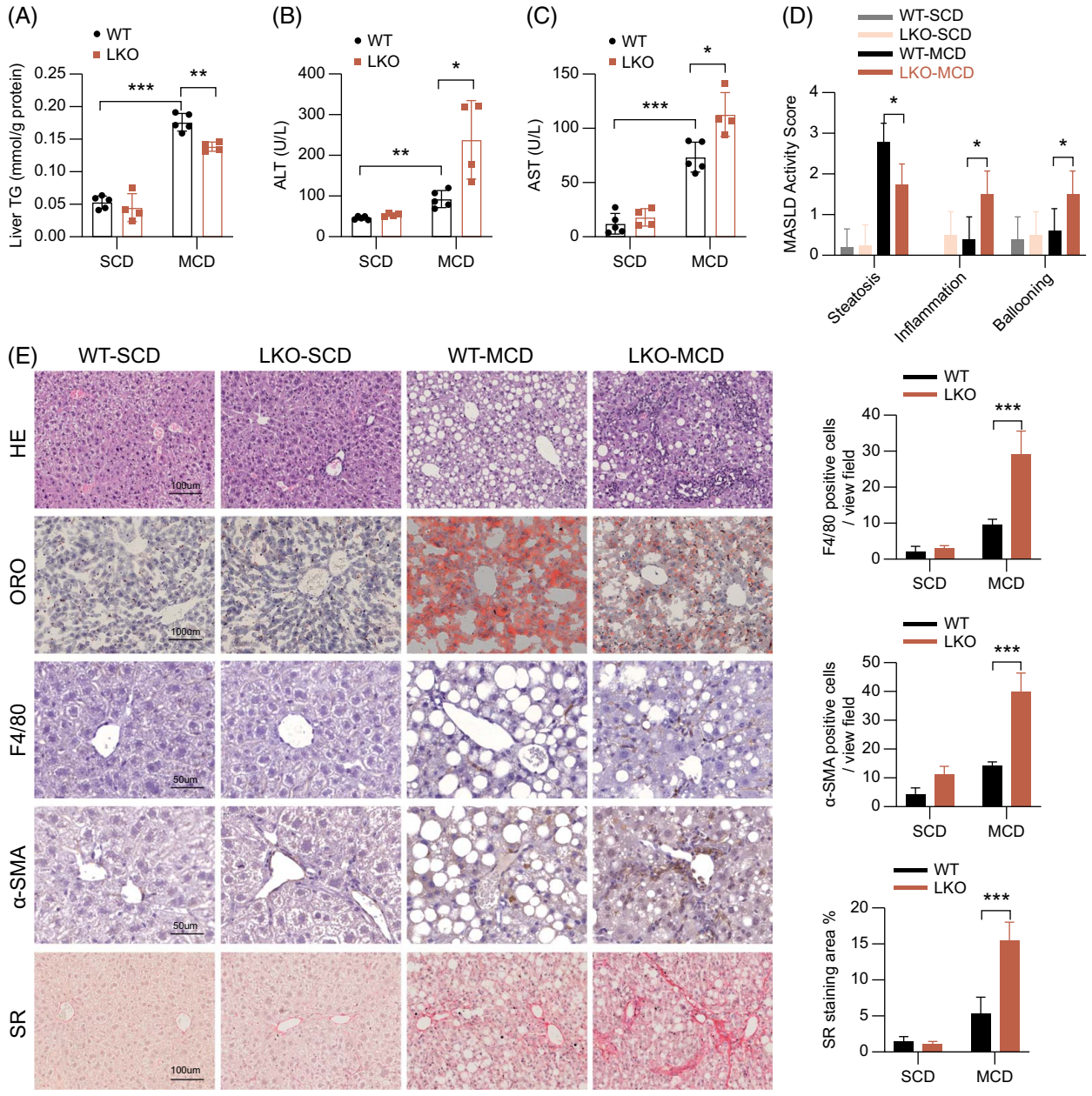

FIGURE 3 Hepatocyte-specific DDB1 deficiency attenuates MCD-induced hepatic steatosis but exacerbates liver injury. (A) Hepatic TG levels in WT and LKO mice fed with SCD or MCD for 4 weeks (n = 5 in WT and n = 4 in LKO). (B, C) Serum ALT and AST levels in the indicated groups after 4 weeks of SCD or MCD feeding. (D, E) Representative HE staining and ORO staining of liver tissues and the corresponding MASLD Activity Scores, and representative IHC staining for F4/80 and α-SMA (scale bar, 50 μm) and SR staining (scale bar, 100 μm) of liver tissues from the indicated groups (n = 5 in WT and n = 4 in LKO). All data are presented as the mean ± SD, $*p < 0.05$, $**p < 0.01$, $***p < 0.001$. Abbreviations: α-SMA, alpha smooth muscle actin; ALT, alanine aminotransferase; AST, aspartate aminotransferase; DDB1, damaged DNA binding protein 1; HE, hematoxylin and eosin; IHC, immunohistochemical; LKO, hepatocyte-specific knockout; MCD, methionine-and choline-deficient diet; ORO, Oil red O; SCD, standard control diet; WT, wild type; SR, Sirius Red.

To systematically assess the involvement of DDB1 in the development of MASH from a transcriptome perspective, we performed RNA sequencing analysis of liver tissues from LKO and WT mice fed with SCD or MCD. GSEA revealed that the occurrence of MASLD was markedly suppressed in the LKO group that was fed the SCD. GSEA-enriched pathways further revealed extensive downregulation of lipid metabolism pathways such as fatty acid elongation, fatty acid degradation, and fatty acid β-oxidation in MCD-fed LKO mice (Supplemental Figure S4A, http://links.lww.com/HC9/A940). However, pathways related to the inflammatory response, extracellular matrix structural constituents, and collagen binding were markedly activated in the MCD-fed LKO group (Supplemental Figure S4B, http://links.lww.com/HC9/A940). Consistently, LKO mice showed significantly downregulated expression of lipid synthesis (*Fasn* and *Scd1*) and uptake (*Cd36*) genes (Supplemental Figure S4C, http://links.lww.com/HC9/A940). *Ddb1*-LKO increased the expression of proinflammatory (*Tnfα, Il6, Ccl2, and Hmgb1*) and fibrotic

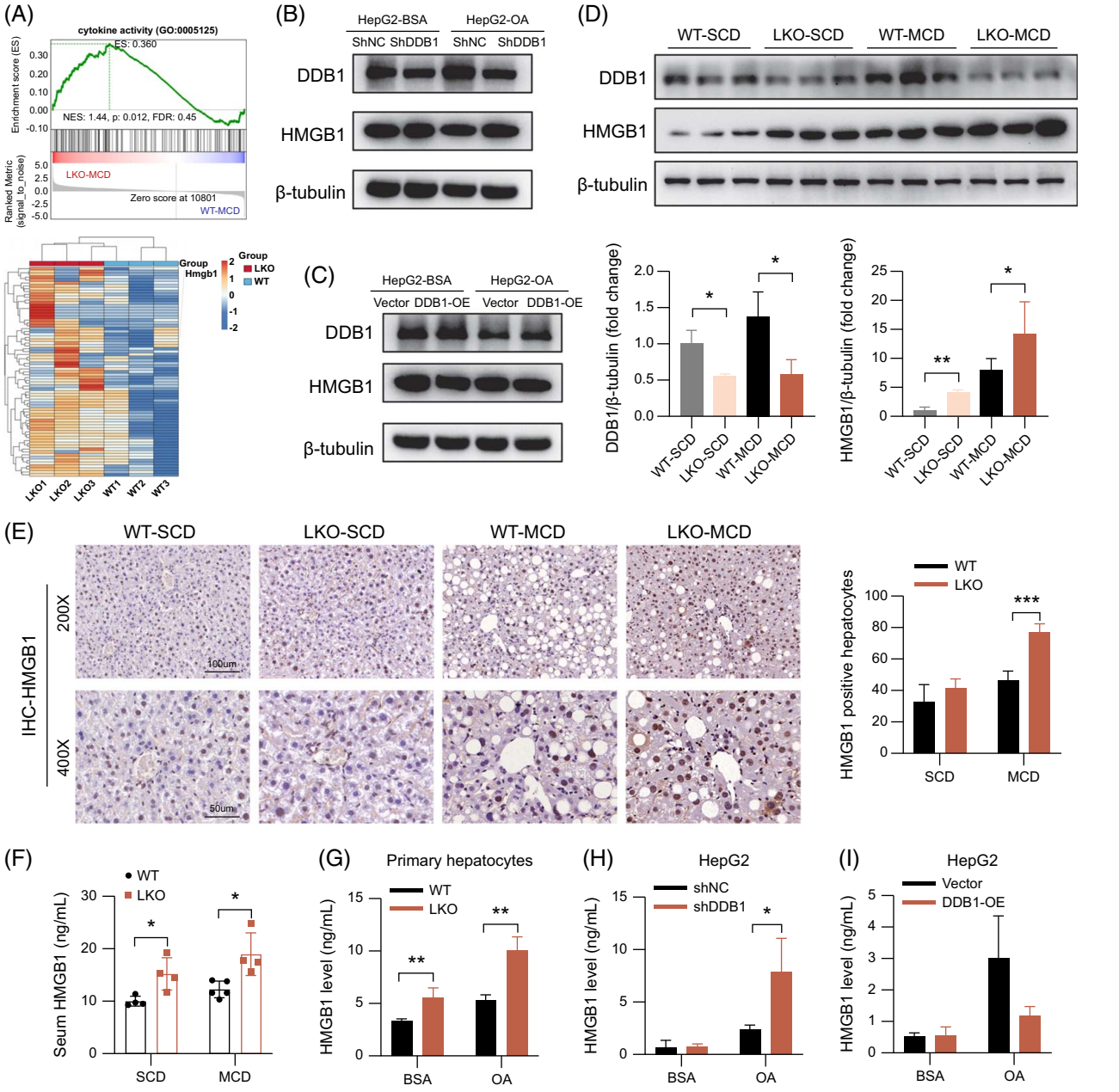

FIGURE 4 HMGB1 was downregulated by DDB1 during MASH. (A) GSEA enriched the pathway related to cytokine activity pathway and the pathway-related gene heatmap in the livers of WT and LKO mice after 4 weeks of SCD or MCD feeding (n = 3 mice per group). (B, C) Protein levels of DDB1 and HMGB1 in HepG2 cells transfected with shDDB1 or DDB1-OE plasmid after BSA or OA stimulation. (D) Western blot and quantitative analysis for protein levels of DDB1 and HMGB1 in WT and LKO mice fed with SCD or MCD for 4 weeks (n = 3 per group). (E) Representative IHC staining and quantitative analysis for HMGB1 in the indicated groups. (F) Serum HMGB1 concentration in the indicated groups was detected by ELISA. (G) Supernatant HMGB1 concentration of primary hepatocytes stimulated with BSA or OA (0.5 mM) for 24 hours. (H, I) Supernatant HMGB1 concentration of HepG2 cells in DDB1 knockdown or overexpressing and their control groups stimulated with BSA or OA (0.5 mM) for 24 hours. All data are presented as the mean ± SD, $^{*}p < 0.05$, $^{**}p < 0.01$, $^{***}p < 0.001$. Abbreviations: BSA, bovine serum albumin; DDB1, damaged DNA binding protein 1; GSEA, gene set enrichment analysis; HMGB1, high-mobility group box 1; IHC, immunohistochemical; LKO, hepatocyte-specific knockout; MCD, methionine-and choline-deficient diet; OA, oleic acid; SCD, standard control diet; WT, wild type.

(*Col1a1, Col3a1, and α-sma*) genes (Supplemental Figures S4D, E, http://links.lww.com/HC9/A940). In general, these results suggest that liver-specific deficiency of DDB1 can alleviate MCD-induced hepatic steatosis but exacerbate MCD-induced liver injury by aggravating hepatocyte damage, facilitating inflammatory responses, and liver fibrosis compared with WT mice.

HMGB1 is downregulated by DDB1 during MASH

Next, we proceeded to reveal the underlying mechanisms involved in the regulatory role of DDB1 in MASH. GSEA-enriched pathways showed that DDB1 deficiency markedly activated cytokine activity pathway-related genes,

including HMGB1 (Figure 4A). HMGB1 is upregulated in MASH and has been shown to mediate the regulation of liver inflammation and fibrosis pathogenesis in mouse models.[18–20] We demonstrated that DDB1 deficiency upregulated *Hmgb1* mRNA expression (Supplemental Figure S4D, http://links.lww.com/HC9/A940). Therefore, we speculated that HMGB1 was a potential target of DDB1 during MASH progression.

We first measured the protein expression of HMGB1 in HepG2 cell models. HMGB1 protein expression was upregulated in shDDB1 cells but was decreased in DDB1-OE cells (Figures 4B, C). Consistently, western blotting confirmed that DDB1 deficiency significantly upregulated the protein levels of HMGB1 in mouse liver tissues (Figure 4D). In addition, the role of DDB1 in regulating HMGB1 expression was validated in an immunohistochemical assay (Figure 4E). Meanwhile, serum HMGB1 concentrations, as well as the concentration of HMGB1 in the supernatants of primary hepatocytes and HepG2 cells, showed that DDB1 deficiency markedly increased the extracellular release of HMGB1 (Figures 4F–I). These findings demonstrate that DDB1 negatively regulates HMGB1 expression and extracellular release.

The function of DDB1 in liver injury depends on HMGB1

Since the final cellular release is correlated with nuclear HMGB1 translocation, western blot analysis was performed using nuclear and cytoplasmic protein lysates to determine whether DDB1 deficiency induces the translocation of HMGB1 from the nucleus to the cytoplasm in hepatocytes (Figures 5A, B). Western blotting demonstrated that when DDB1 was deficient, HMGB1 expression was increased in both the nucleus and the cytoplasm, with the cytoplasmic increase being more pronounced. This indicated that DDB1 deletion promoted the nuclear translocation of HMGB1 to some extent. In addition, HMGB1 can be passively released from necrotic cells. The declined viability of DDB1-deficient hepatocytes also facilitated the extracellular release of HMGB1 (Figures 2E, L). These results motivated us to investigate whether DDB1 functioned through HMGB1 to regulate liver injury. In OA-treated HepG2 cells, HMGB1 silencing successfully reversed the suppressive effects of DDB1 silencing on cell viability but had few effects on lipid deposition (Figures 5C–E). Moreover, in OA-treated primary hepatocytes, we confirmed that HMGB1 depletion abolished the cell damage induced by DDB1 deficiency under OA stress (Figures 5F–H).

To further demonstrate the contribution of HMGB1 to the effect of DDB1 on MASH in vivo, we induced *Hmgb1* knockdown (KD) in livers of WT and LKO mice with AAV8-shHmgb1. EGFP labeling and western blotting verified that the expression of HMGB1 was abolished in the liver tissues of WT-KD and LKO-KD mice (Supplemental Figures S5A–D, Supplemental Digital Content 1, http://links.lww.com/HC9/A940). Consistent with the findings in vitro, hepatic steatosis was slightly altered, but the increased levels of serum ALT and AST in LKO mice were abolished in LKO-KD mice (Figures 6A–E). Hematoxylin and eosin and Sirius Red staining showed that *Hmgb1* KD successfully reversed DDB1 deficiency-induced liver inflammation and fibrosis. Moreover, histological staining showed that HMGB1 depletion abrogated the activation of macrophages and HSCs (Figures 6F, G). Collectively, these findings suggest that HMGB1 is crucial to the regulatory effects of DDB1 deficiency on liver injury and fibrosis.

DDB1 and HMGB1 expression in human MASH cohort

Considering that MCD-induced liver injury is not entirely identical to clinical MASH, we selected 39 control, MASLD, and MASH human samples for RNA sequencing to further verify the role of the DDB1-HMGB1 axis in patients with MASH. We divided patients into 2 groups based on inflammation scores and 3 groups based on fibrosis scores. The results showed that with the increase of inflammation and fibrosis, DDB1 expression was significantly reduced, while HMGB1 expression was significantly increased (Figures 7A–F). In addition, the expression pattern further confirmed that DDB1 negatively regulates HMGB1 more significantly (Figure 7G). In summary, DDB1 plays a dual role in the development of hepatic steatosis and injury. DDB1 deficiency attenuates hepatic steatosis by downregulating the expression of lipid metabolism genes. However, DDB1 deficiency upregulates the expression and extracellular release of HMGB1, which further exacerbates hepatocyte damage, increases KC infiltration, and activates HSCs, ultimately leading to aggravated liver inflammation and fibrosis (Figure 7H).

DISCUSSION

The present study uncovered a previously unknown role of DDB1 in MASH pathogenesis. We observed that DDB1 expression was significantly decreased in the livers of humans and mice with MASH. To investigate the biological effects of DDB1 downregulation, we obtained *Ddb1*-LKO mice. Unexpectedly, MCD-fed LKO mice developed severe cell damage, inflammation, and fibrosis despite a reduction in hepatic steatosis. We further identified HMGB1 as a candidate target by which DDB1 regulates inflammation and fibrosis.

The clinical outcomes of MASLD and MASH are markedly heterogeneous, so the 2 subgroups correspond

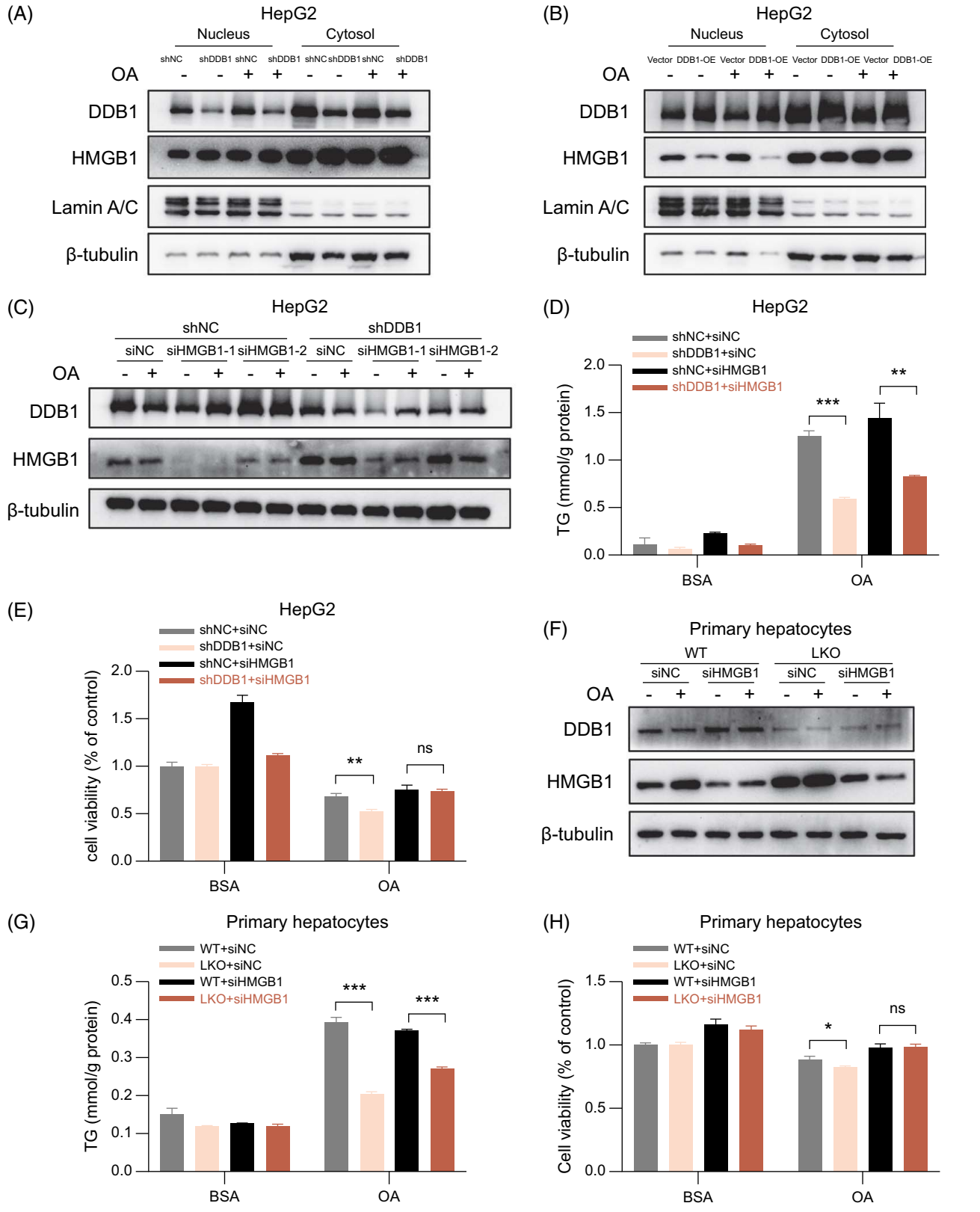

FIGURE 5 The function of DDB1 in cell damage depends on HMGB1. (A, B) Western blot analysis of nuclear and cytoplasmic protein lysates of HepG2 cells in DDB1 knockdown or overexpressing and their control groups stimulated with BSA or OA (0.5 mM) for 24 hours. (C) Western blotting of DDB1 and HMGB1 in HepG2 shNC and shDDB1 cells transfected with siRNA or siHMGB1 and stimulated with BSA or OA (0.5 mM) for 24 hours. (D) The cellular contents of TG in the indicated HepG2 cell groups. (E) CCK8 analysis of HepG2 cell viability in the indicated groups. (F) Western blotting of DDB1 and HMGB1 in primary hepatocytes transfected with siRNA or siHMGB1 and stimulated with BSA or OA (0.5 mM) for 24 hours. (G) The cellular contents of TG in the indicated primary hepatocyte groups. (H) CCK8 analysis of primary hepatocyte viability in the indicated groups. All data are presented as the mean ± SD, $*p < 0.05$, $**p < 0.01$, $***p < 0.001$. Abbreviations: BSA, bovine serum albumin; DDB1, damaged DNA binding protein 1; HMGB1, high-mobility group box 1; OA, oleic acid; TG, triglycerides.

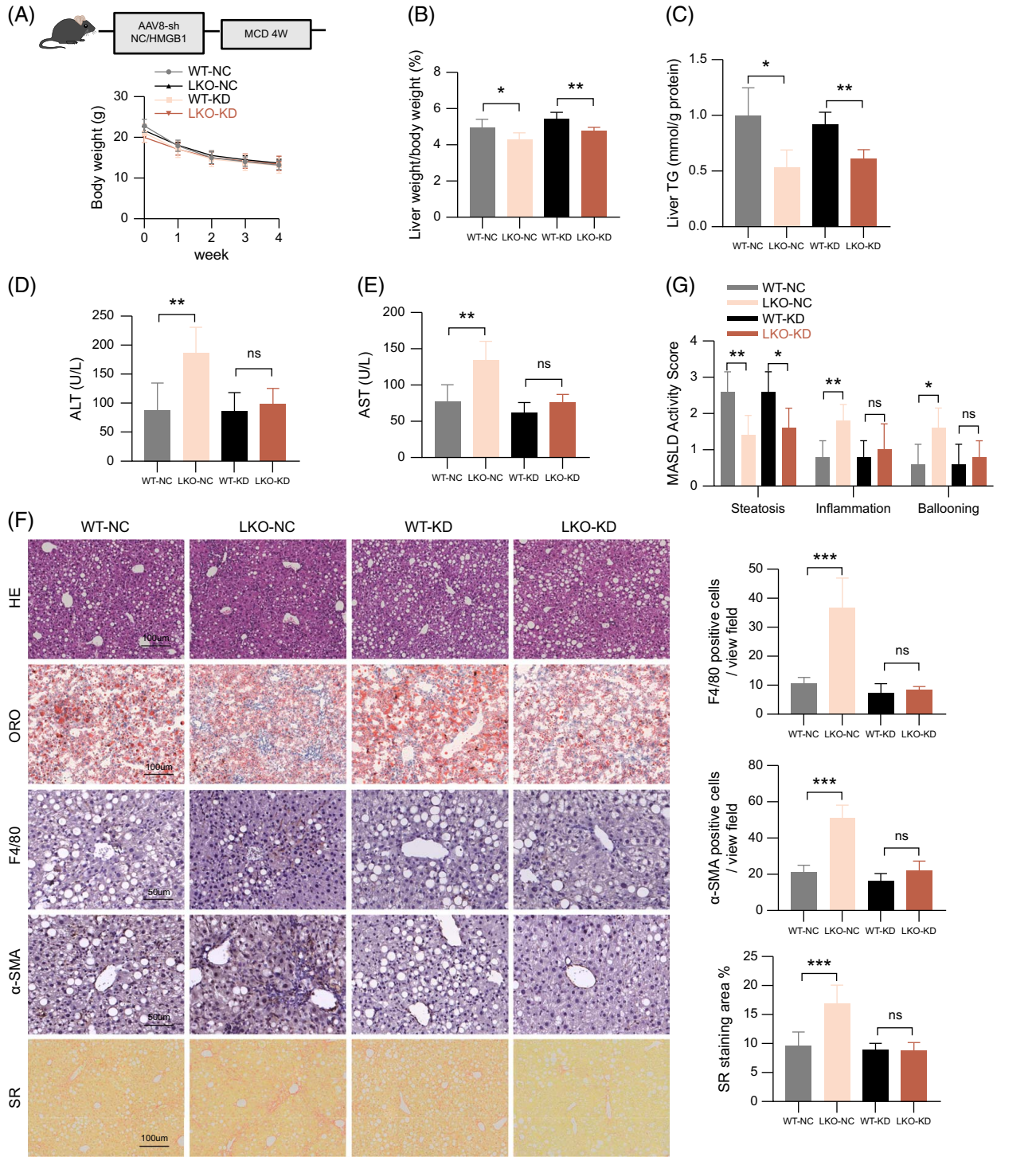

FIGURE 6 The function of DDB1 in liver inflammation and fibrosis depends on HMGB1. (A) Body weight changes during 4 weeks of MCD feeding in WT and LKO mice received i.v. injection of AAV8-shNC or AAV8-shHmgb1 (n = 5 per group). (B) Liver-weight-to-body-weight ratio in the indicated groups after 4 weeks of MCD feeding. (C) Hepatic TG levels in the indicated groups. (D, E) Serum ALT and AST levels in the indicated groups. (F) Representative images of liver sections stained with HE (scale bar, 100 μm), ORO (scale bar, 100 μm), IHC for F4/80 and α-SMA (scale bar, 50 μm), and SR (scale bar, 100 μm). (G) The corresponding quantitative analysis in the indicated groups. All data are presented as the mean ± SD, *$p < 0.05$, **$p < 0.01$, ***$p < 0.001$. Abbreviations: α-SMA, alpha smooth muscle actin; ALT, alanine aminotransferase; AST, aspartate aminotransferase; DDB1, damaged DNA binding protein 1; HE, hematoxylin and eosin; HMGB1, high-mobility group box 1; IHC, immunohistochemical; LKO, hepatocyte-specific knockout; MCD, methionine-and choline-deficient diet; ORO, Oil red O; WT, wild type.

to separate entities.[21] MASH is a proven risk factor for advanced liver outcomes, including cirrhosis, HCC, and liver transplantation.[22] Inflammation and fibrosis are considered to be key processes that promote MASH to cirrhosis and hepatocarcinogenesis.[23,24] Many factors are involved in the development of MASH, and genetic

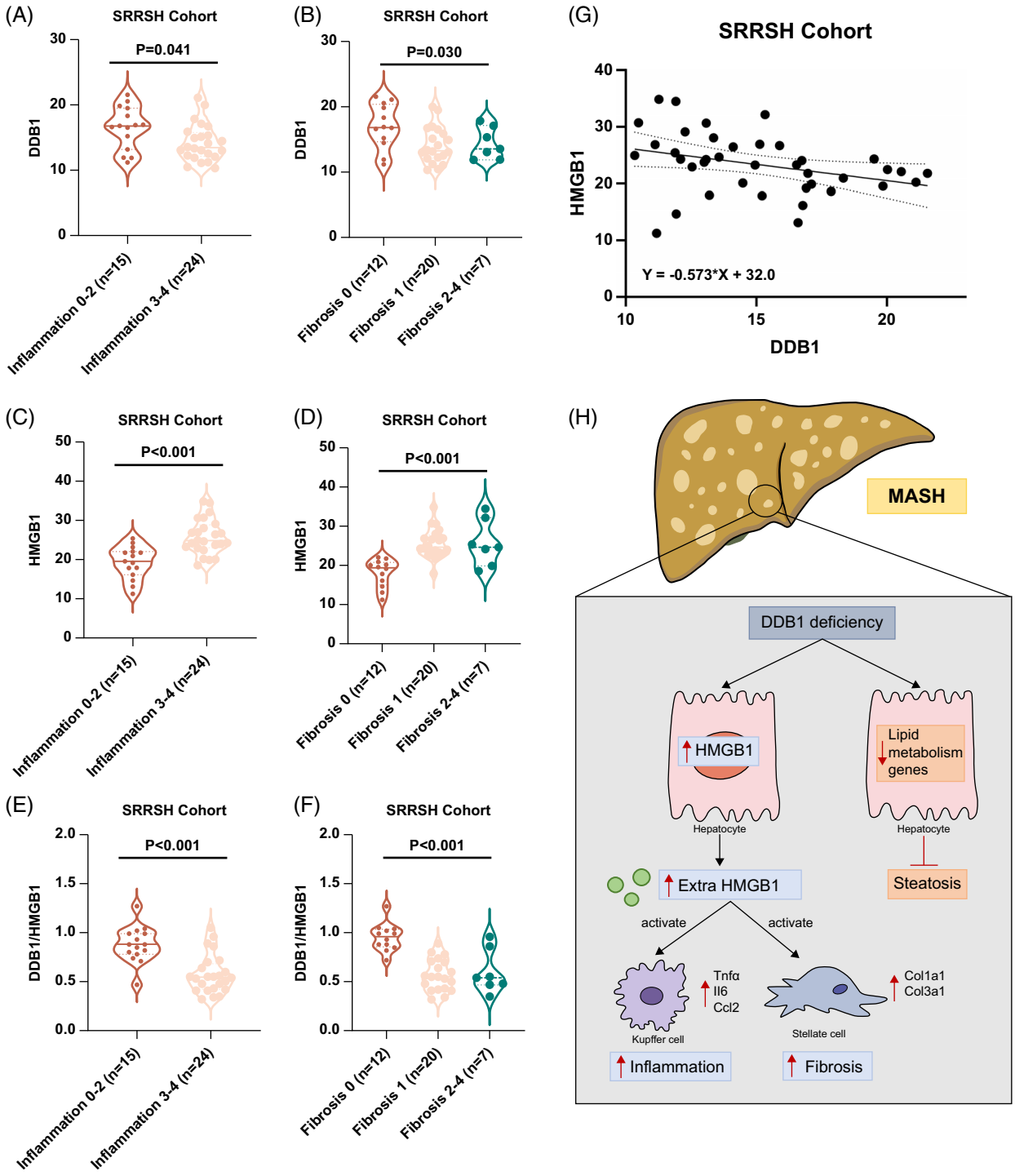

FIGURE 7 DDB1 and HMGB1 expression in human MASH cohort. (A) The expression of DDB1 in the inflammatory group (n = 15 in the inflammation 0–2 group and n = 24 in the inflammation 3–4 group). (B) The expression of DDB1 in the fibrosis group (n = 12 in the fibrosis 0 group, n = 20 in the fibrosis 1 group, and n = 7 in the fibrosis 2–4 group). (C) The expression of HMGB1 in the inflammatory group (n = 15 in the inflammation 0–2 group and n = 24 in the inflammation 3–4 group). (D) The expression of HMGB1 in the fibrosis group (n = 12 in the fibrosis 0 group, n = 20 in the fibrosis 1 group, and n = 7 in the fibrosis 2–4 group). (E) The ratio of DDB1 and HMGB1 in the inflammatory group (n = 15 in the inflammation 0–2 group and n = 24 in the inflammation 3–4 group). (F) The ratio of DDB1 and HMGB1 in the fibrosis group (n = 12 in the fibrosis 0 group, n = 20 in the fibrosis 1 group, and n = 7 in the fibrosis 2–4 group). (G) The negative expression of DDB1 and HMGB1. (H) The Mechanism diagram. Abbreviations: DDB1, damaged DNA binding protein 1; HMGB1, high-mobility group box 1.

polymorphisms have been shown to influence its progression.[25–28] It has been reported that DDB1 is involved in the regulation of multiple genes as a transcription factor partner, such as E2F1-activated genes,[9] UV-induced fibromodulin,[29] and genes with HomoID-containing promoters.[30] A recent report

revealed a critical role of DDB1 and BRWD3 as a transcriptional complex in adipogenesis and the onset of obesity.[13] Particularly, the function of DDB1 in HCC has received extensive attention.[31–33] Therefore, investigating the unknown role of DDB1 in the pathophysiology of MASH is of both clinical and scientific interest.

Here, we found that DDB1 levels were significantly reduced during the progression of MASH in humans and mice. To examine the function of DDB1 in the development of MASH, we challenged WT and LKO mice with MCD, which is the favored approach to research MASH pathogenesis. Although the MCD diet has some drawbacks, such as causing weight loss and lack of systemic insulin resistance,[34] it is more effective and repeatable in inducing severe liver injury and progressive fibrosis and is suitable for researching the mechanisms underlying MASH-related inflammation and fibrosis as well as strategies for preventing these conditions, compared to the HFD diet.[35,36]

Notably, we provide direct evidence that DDB1 plays dual roles in the progression of hepatic steatosis and injury. It is generally believed that during nonalcoholic liver injury, the accumulation of TG in hepatocytes is the first step that leads to inflammation and lipotoxicity.[37] In our study, however, MCD-fed LKO mice had less steatosis than WT mice but had increased liver injury, suggesting independence between hepatic steatosis and injury. This notion has also been supported by an increasing number of studies.[38–41] For example, Kawamura et al[38] reported that inhibiting SREBP-mediated lipogenesis unexpectedly exacerbated liver damage and carcinogenesis in a mouse MASH model. In addition, Yamaguchi et al[42] reported that blocking TG synthesis attenuated steatosis but aggravated liver injury and fibrosis. The researchers demonstrated that TG was not hepatotoxic in MCD-induced MASH mice and protected hepatocytes from lipotoxicity by reducing free fatty acid accumulation. These findings are consistent with our results. Considering the suppressive effects of DDB1 on hepatic inflammation and fibrosis, it is reasonable to expect that DDB1 may be a promising therapeutic target to prevent the progression of MASH.

In the current study, we identified HMGB1 as a downstream target of DDB1, which critically mediated the regulatory roles of DDB1 in hepatic inflammation and fibrosis. HMGB1, which is a prototypical damage-associated molecular pattern, has attracted much attention for promoting the inflammatory response and fibrosis in MASH.[20] HMGB1 is ubiquitously expressed in parenchymal and nonparenchymal hepatic cells, and hepatocytes were proven to be the main hepatic cellular source of HMGB1 in MASH.[18,43] It is well known that HMGB1 can promote the conversion of liver macrophages into the proinflammatory M1 phenotype, thus causing an inflammatory response.[44] Moreover, HMGB1 activates HSCs to stimulate liver fibrosis.[45] Ge[18] reported that increases in HMGB1 expression and secretion aggravated the degree of liver fibrosis in mice. In this study, we demonstrated that DDB1 negatively regulated HMGB1 expression and extracellular release to a large extent. HMGB1 depletion indeed reduced macrophage infiltration and suppressed stellate cell activation. We confirmed that suppressing HMGB1 could not reverse the effects of DDB1 deficiency on regulating lipid deposition but that HMGB1 was crucial for the regulation of DDB1 deficiency-induced inflammatory response and fibrosis induced in vivo and in vitro. The regulation of DDB1 on lipid deposition is mainly achieved by changing enzymes related to lipid metabolism, which also explains, to some extent, the nonparallel relationship between hepatic steatosis and liver injury. Thus, we identified HMGB1 as a downstream target of DDB1 regulating liver injury in MASH, which critically mediates the regulatory role of DDB1 in liver inflammation and fibrosis. However, the underlying mechanism by which DDB1 regulates HMGB1 needs to be further clarified and confirmed by follow-up studies.

In summary, the present data provide evidence of a dissociation between the attenuation of steatosis and exacerbation of liver injury. DDB1 deletion inhibited lipogenesis but unexpectedly aggravated liver inflammation and fibrosis by increasing HMGB1 expression and extracellular release. These findings have significant ramifications for the development of therapeutic strategies for MASH.

DATA AVAILABILITY STATEMENT

The datasets used and/or analyzed in this paper have been deposited in the OMIX, China National Center for Bioinformation/Beijing Institute of Genomics, Chinese Academy of Sciences (https://ngdc.cncb.ac.cn/omix; accession no.OMIX005613/OMIX005620).

AUTHOR CONTRIBUTIONS

Xiujun Cai and Yifan Tong designed the research. Qiuxia Gu and Yushun Chang performed experiments, analyzed data, and wrote the main manuscript. Yan Jin, Jie Lin, and Xi Zhu performed the semiquantitative analysis. Jing Fang, Binzhi Dong, Hanning Ying, and Zerui Gao drew the mechanism diagram. Xiaoxiao Fan, Zheyong Li, and Yongfen Zhu revised and supplemented the manuscript. All authors read and approved the submitted version.

ACKNOWLEDGMENTS

The authors thank Prof Yong Cang, ShanghaiTech University, for providing the *Ddb1*$^{flox/flox}$ mice and Albumin-Cre$^{+/-}$ mice and Prof Zheng Fenping, Zhejiang University, for providing the liver samples from leptin receptor deletion mice (db/db) and control group (db/m).

FUNDING INFORMATION

This study was supported by the Zhejiang Provincial Natural Science Foundation of China (Grant Nos.

LY23H030006 and LQ21H030012) and the National Natural Science Foundation of China (Grant No. 82200672).

CONFLICTS OF INTEREST

The authors have no conflicts to report.

ORCID

Qiuxia Gu https://orcid.org/0000–0003–0176–5008
Yifan Tong https://orcid.org/0000–0001–9028–5756

REFERENCES

1. Younossi ZM, Koenig AB, Abdelatif D, Fazel Y, Henry L, Wymer M. Global epidemiology of nonalcoholic fatty liver disease—Meta-analytic assessment of prevalence, incidence, and outcomes. Hepatology. 2016;64:73–84.
2. Younossi ZM. Non-alcoholic fatty liver disease—A global public health perspective. J Hepatol. 2019;70:531–44.
3. Kanwal F, Shubrook JH, Younossi Z, Natarajan Y, Bugianesi E, Rinella ME, et al. Preparing for the NASH epidemic: A call to action. Gastroenterology. 2021;161:1030–42.e1038.
4. Friedman SL, Neuschwander-Tetri BA, Rinella M, Sanyal AJ. Mechanisms of NAFLD development and therapeutic strategies. Nat Med. 2018;24:908–22.
5. Anstee QM, Reeves HL, Kotsiliti E, Govaere O, Heikenwalder M. From NASH to HCC: Current concepts and future challenges. Nat Rev Gastroenterol Hepatol. 2019;16:411–28.
6. Newsome PN, Buchholtz K, Cusi K, Linder M, Okanoue T, Ratziu V, et al. A placebo-controlled trial of subcutaneous semaglutide in nonalcoholic steatohepatitis. N Engl J Med. 2021;384:1113–24.
7. Chu G, Yang W. Here comes the sun: Recognition of UV-damaged DNA. Cell. 2008;135:1172–4.
8. Lee J, Zhou P. DCAFs, the missing link of the CUL4-DDB1 ubiquitin ligase. Mol Cell. 2007;26:775–80.
9. Hayes S, Shiyanov P, Chen X, Raychaudhuri P. DDB, a putative DNA repair protein, can function as a transcriptional partner of E2F1. Mol Cell Biol. 1998;18:240–9.
10. Datta A, Bagchi S, Nag A, Shiyanov P, Adami GR, Yoon T, et al. The p48 subunit of the damaged-DNA binding protein DDB associates with the CBP/p300 family of histone acetyltransferase. Mutat Res. 2001;486:89–97.
11. Iovine B, Iannella ML, Bevilacqua MA. Damage-specific DNA binding protein 1 (DDB1): A protein with a wide range of functions. Int J Biochem Cell Biol. 2011;43:1664–7.
12. Tong X, Zhang D, Charney N, Jin E, VanDommelen K, Stamper K, et al. DDB1-mediated CRY1 degradation promotes FOXO1-driven gluconeogenesis in liver. Diabetes. 2017;66:2571–82.
13. Wang X, Wang HY, Hu GS, Tang WS, Weng L, Zhang Y, et al. DDB1 binds histone reader BRWD3 to activate the transcriptional cascade in adipogenesis and promote onset of obesity. Cell Rep. 2021;35:109281.
14. Tong X, Zhang D, Shabandri O, Oh J, Jin E, Stamper K, et al. DDB1 E3 ligase controls dietary fructose-induced ChREBPα stabilization and liver steatosis via CRY1. Metabolism. 2020;107:154222.
15. Bedossa P, Poitou C, Veyrie N, Bouillot JL, Basdevant A, Paradis V, et al. Histopathological algorithm and scoring system for evaluation of liver lesions in morbidly obese patients. Hepatology. 2012;56:1751–9.
16. Li G, Ji T, Chen J, Fu Y, Hou L, Feng Y, et al. CRL4(DCAF8) ubiquitin ligase targets histone H3K79 and promotes H3K9 methylation in the liver. Cell Rep. 2017;18:1499–511.
17. Lee H. Obesity-associated cancers: Evidence from studies in mouse models. Cells. 2022;11:1472.
18. Ge X, Arriazu E, Magdaleno F, Antoine DJ, Dela Cruz R, Theise N, et al. High mobility group box-1 drives fibrosis progression signaling via the receptor for advanced glycation end products in mice. Hepatology. 2018;68:2380–404.
19. Li L, Chen L, Hu L, Liu Y, Sun HY, Tang J, et al. Nuclear factor high-mobility group box1 mediating the activation of Toll-like receptor 4 signaling in hepatocytes in the early stage of nonalcoholic fatty liver disease in mice. Hepatology. 2011;54:1620–30.
20. Khambu B, Yan S, Huda N, Yin XM. Role of high-mobility group box-1 in liver pathogenesis. Int J Mol Sci. 2019;20:5314.
21. Arab JP, Arrese M, Trauner M. Recent insights into the pathogenesis of nonalcoholic fatty liver disease. Annu Rev Pathol. 2018;13:321–50.
22. Machado MV, Diehl AM. Pathogenesis of nonalcoholic steatohepatitis. Gastroenterology. 2016;150:1769–77.
23. Arrese M, Cabrera D, Kalergis AM, Feldstein AE. Innate immunity and inflammation in NAFLD/NASH. Dig Dis Sci. 2016;61:1294–303.
24. Friedman SL. Liver fibrosis in 2012: Convergent pathways that cause hepatic fibrosis in NASH. Nat Rev Gastroenterol Hepatol. 2013;10:71–2.
25. Zhao Y, Gao L, Jiang C, Chen J, Qin Z, Zhong F, et al. The transcription factor zinc fingers and homeoboxes 2 alleviates NASH by transcriptional activation of phosphatase and tensin homolog. Hepatology. 2022;75:939–54.
26. Yan L, Zhang T, Wang K, Chen Z, Yang Y, Shan B, et al. SENP1 prevents steatohepatitis by suppressing RIPK1-driven apoptosis and inflammation. Nat Commun. 2022;13:7153.
27. Vesting AJ, Jais A, Klemm P, Steuernagel L, Wienand P, Fog-Tonnesen M, et al. NIK/MAP3K14 in hepatocytes orchestrates NASH to hepatocellular carcinoma progression via JAK2/STAT5 inhibition. Mol Metab. 2022;66:101626.
28. Eslam M, Valenti L, Romeo S. Genetics and epigenetics of NAFLD and NASH: Clinical impact. J Hepatol. 2018;68:268–79.
29. Bevilacqua MA, Iovine B, Zambrano N, D'Ambrosio C, Scaloni A, Russo T, et al. Fibromodulin gene transcription is induced by ultraviolet irradiation, and its regulation is impaired in senescent human fibroblasts. J Biol Chem. 2005;280:31809–17.
30. Contreras-Levicoy J, Moreira-Ramos S, Rojas DA, Urbina F, Maldonado E. Transcription directed by human core promoters with a HomolD box sequence requires DDB1, RECQL and RNA polymerase II machinery. Gene. 2012;505:318–23.
31. Martin-Lluesma S, Schaeffer C, Robert EI, van Breugel PC, Leupin O, Hantz O, et al. Hepatitis B virus X protein affects S phase progression leading to chromosome segregation defects by binding to damaged DNA binding protein 1. Hepatology. 2008;48:1467–76.
32. Leupin O, Bontron S, Schaeffer C, Strubin M. Hepatitis B virus X protein stimulates viral genome replication via a DDB1-dependent pathway distinct from that leading to cell death. J Virol. 2005;79:4238–45.
33. Yu M, Chen Z, Zhou Q, Zhang B, Huang J, Jin L, et al. PARG inhibition limits HCC progression and potentiates the efficacy of immune checkpoint therapy. J Hepatol. 2022;77:140–51.
34. Santhekadur PK, Kumar DP, Sanyal AJ. Preclinical models of non-alcoholic fatty liver disease. J Hepatol. 2018;68:230–7.
35. Wu S, Wang X, Xing W, Li F, Liang M, Li K, et al. An update on animal models of liver fibrosis. Front Med (Lausanne). 2023;10:1160053.
36. Alshawsh MA, Alsalahi A, Alshehade SA, Saghir SAM, Ahmeda AF, Al Zarzour RH, et al. A comparison of the gene expression profiles of non-alcoholic fatty liver disease between animal models of a high-fat diet and methionine-choline-deficient diet. Molecules. 2022;27:858.
37. Day CP, James OF. Steatohepatitis: A tale of two "hits"? Gastroenterology. 1998;114:842–5.

38. Kawamura S, Matsushita Y, Kurosaki S, Tange M, Fujiwara N, Hayata Y, et al. Inhibiting SCAP/SREBP exacerbates liver injury and carcinogenesis in murine nonalcoholic steatohepatitis. J Clin Invest. 2022;132:e151895.
39. Lee YS, Kim DY, Kim TJ, Kim SY, Jeong JM, Jeong WI, et al. Loss of toll-like receptor 3 aggravates hepatic inflammation but ameliorates steatosis in mice. Biochem Biophys Res Commun. 2018;497:957–62.
40. Fuchs CD, Krivanec S, Steinacher D, Mlitz V, Wahlström A, Stahlman M, et al. Absence of Bsep/Abcb11 attenuates MCD diet-induced hepatic steatosis but aggravates inflammation in mice. Liver Int. 2020;40:1366–77.
41. Yamaguchi K, Itoh Y, Yokomizo C, Nishimura T, Niimi T, Fujii H, et al. Blockade of interleukin-6 signaling enhances hepatic steatosis but improves liver injury in methionine choline-deficient diet-fed mice. Lab Invest. 2010;90:1169–78.
42. Yamaguchi K, Yang L, McCall S, Huang J, Yu XX, Pandey SK, et al. Inhibiting triglyceride synthesis improves hepatic steatosis but exacerbates liver damage and fibrosis in obese mice with nonalcoholic steatohepatitis. Hepatology. 2007;45:1366–74.
43. Lin M, Long J, Li W, Yang C, Loughran P, O'Doherty R, et al. Hepatocyte high-mobility group box 1 protects against steatosis and cellular stress during high fat diet feeding. Mol Med. 2020;26:115.
44. Li Z, Fu WJ, Chen XQ, Wang S, Deng RS, Tang XP, et al. Autophagy-based unconventional secretion of HMGB1 in glioblastoma promotes chemosensitivity to temozolomide through macrophage M1-like polarization. J Exp Clin Cancer Res. 2022;41:74.
45. Xue J, Suarez JS, Minaai M, Li S, Gaudino G, Pass HI, et al. HMGB1 as a therapeutic target in disease. J Cell Physiol. 2021;236:3406–19.

How to cite this article: Gu Q, Chang Y, Jin Y, Fang J, Ji T, Lin J, et al. Hepatocyte-specific loss of DDB1 attenuates hepatic steatosis but aggravates liver inflammation and fibrosis in MASH. Hepatol Commun. 2024;8:e0474. https://doi.org/10.1097/HC9.0000000000000474